*Journal of Sound and Vibration* (2002) **254**(3), 557–573
doi:10.1006/jsvi.2001.4110, available online at http://www.idealibrary.com on IDEAL®

# EFFECT OF GRAZING–BIAS FLOW INTERACTION ON ACOUSTIC IMPEDANCE OF PERFORATED PLATES

X. Sun, X. Jing, H. Zhang and Y. Shi

*Department of Jet Propulsion, Beijing University of Aeronautics and Astronautics,* 100083 *Beijing, People's Republic of China. E-mail: sunxf@buaa.edu.cn*

(*Received* 15 *June* 2001, *and in final form* 19 *November* 2001)

In this paper, the effect of grazing–bias flow interaction on the acoustic behavior of a perforated plate is investigated. In the experiment, bias flow into or out of orifices (inflow or outflow) is used to change the acoustic impedance of the test perforated plates subjected to grazing flow, and the acoustic impedance is measured as a function of both grazing and bias flow speeds. A comparison is made between the present measured orifice acoustic resistance and the previous results for steady state orifice resistance. Qualitatively, both results show similar characteristics. It is shown that there is some difference between grazing-inflow and grazing-outflow interactions. In the outflow case, grazing flow results in the drop of the acoustic resistance below the non-grazing flow value at high bias flow speed, whereas it generally has the effect of increasing the acoustic resistance in the inflow case. Furthermore, a simple grazing–bias flow interaction model is set up in an attempt to explain the observed phenomena. This model shows that the acoustic resistance of an orifice in a thin plate is proportional to bias flow Mach number, and is inverse to the square of the effective discharge coefficient which depends only on the ratio of bias flow speed to grazing flow speed. Finally, based on the theoretical analysis and the experimental data, an empirical equation is presented for the effective discharge coefficient.



## 1. INTRODUCTION

An acoustic liner of perforated type is applied extensively to suppress noise and combustion instabilities. In traditional applications an acoustic liner passively absorbs noise, thus its performance is very sensitive to environments, such as noise frequency and mean flow conditions. In order to overcome this limitation, Dean and Tester [1] proposed a novel concept of "tunable" acoustic liner. Recently, facing the pressing need for quiet aeroengines, researchers have paid lot of attention on a kind of passive/active hybrid noise control technique based on Dean and Tester's concept. In addition, more recent work [2, 3] indicates that it is possible to use this type of tunable acoustic liner as casing treatment to realize the active control of the cascade flutter.

In the applications mentioned above, the acoustic liner encounters two mean flow conditions. Grazing flow over the surface of an acoustic liner would always be present. There would also be bias flow through the orifices for cooling purpose when an acoustic liner is used to suppress combustion instabilities. In the Dean and Tester [1] concept, bias flow through the orifices is deliberately introduced, and the liner impedance is controlled by varying bias flow speed. In the situation of zero grazing flow and normally incident sound, the work of Hughes and Dowling [4], and Zhao and Sun [5] makes evident the high performance of the tunable acoustic liner with bias flow. Recently, more realistic experiments in which this type of tunable acoustic liner is used in a flow duct were carried

0022-460X/02/$35.00 

out by Kwan *et al.* [6], and Cataldi *et al.* [7]. In reference [7], bias flow into or out of a liner (inflow or outflow) is used for controlling the liner impedance with grazing flow being present. Their experimental results show that the effectiveness of this type of tunable liner is affected by not only the grazing flow speed but also the bias flow direction. Although the underlying physics of these phenomena is still not very clear, it is reasonable to deduce that the interaction of grazing flow with bias flow will affect the way in which bias flow changes the liner impedance, thereby resulting in the variation of the noise attenuation in the flow duct. As noted by Dean and Tester [1], the effect of grazing flow on the duct-facing layer of the acoustic liner is one of the major complications which exist in the application of the proposed concept. Thus, a clear and detailed understanding of the effect of grazing–bias flow interaction is not only essential for the design of high-efficiency acoustic liner for suppressing combustion instabilities, but also a crucial step towards the practical application of the passive/active hybrid noise control technique.

The mean flow effects on the liner impedance have long attracted the attention of the researchers. However, in most of the previous studies, the effects of the two mean flow conditions—grazing flow and bias flow are separately considered. On the one hand, grazing flow effect on the liner impedance has been studied in detail by Rice [8], Kompenhans and Ronneberger [9], Walker and Charwat [10], Cummings [11], Howe *et al.* [12, 13], and Jing *et al.* [14]; on the other hand, bias flow effect has been investigated to some success by Bechert [15], Ingard and Ising [16], Howe [17], Cummings and Eversman [18], Salikuddin and Ahuja [19], Jing and Sun [20]. Lewis and Garrison [21] tried to incorporate both grazing flow and bias flow effects into their empirical impedance model, but basically the two effects are independently treated. It is obvious that what we are concerned with here is how the interaction between grazing and bias flow rather than each independently affects the liner impedance. To the authors' knowledge, so far few efforts have been made on this problem. Rogers and Hersh [22] presented an investigation of the interaction between grazing and orifice flow, but only steady state orifice resistance is considered in their work. It is believed that there is some connection between steady state and acoustic resistance of an orifice. For instance, the non-linear acoustic resistance of an orifice at high SPL can be well approximated by the steady state orifice resistance. However, when grazing flow interacts with bias flow, it would be expected that a more complicated situation arises. Detailed investigation is needed before concluding as to whether there is such an equivalence relation or not in the case of grazing–bias flow interaction.

This paper investigates the effect of grazing–bias flow interaction on the liner acoustic impedance. First, an experimental set-up is established to measure the acoustic impedance of the test perforated plates subjected to both grazing and bias flow. Bias flow used for adjusting the acoustic impedance of a test perforated plate is introduced in two different ways: inflow and outflow. Furthermore, a simple grazing–bias flow interaction model is set up in order to provide more insight into the experimental results. This model shows that the acoustic resistance of an orifice in a thin plate is proportional to bias flow Mach number, and is inverse to the square of the effective discharge coefficient which depends only on the ratio of bias flow speed to grazing flow speed. Finally, on the basis of the experiment and the theory an empirical equation is obtained for the effective discharge coefficient.

## 2. EXPERIMENTAL SET-UP AND RELIABILITY TEST

### 2.1. EXPERIMENTAL SET-UP

In the present experiment, we use a two-microphone technique to measure the acoustic impedance of a perforated plate subjected to both grazing flow and bias flow. The

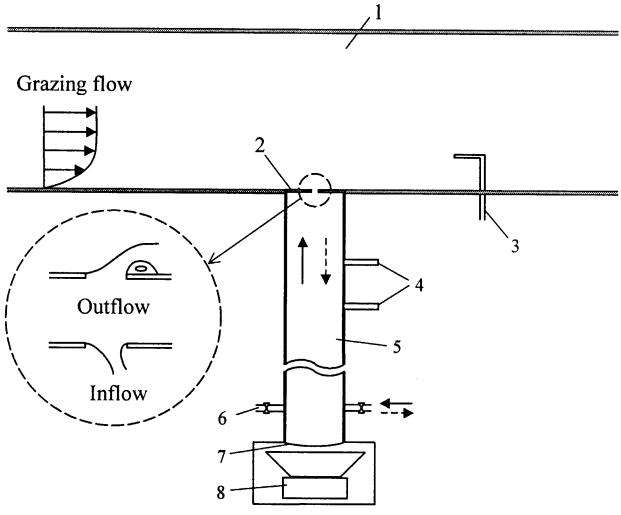


Figure 1. Schematic of the experimental set-up. 1, wind tunnel; 2, test perforated plate; 3, Pitot-static tube; 4, microphones; 5, impedance tube; 6, air inlets for bias flow; 7, membrane; 8, loudspeaker. Arrows indicate the flow direction in the impedance tube.

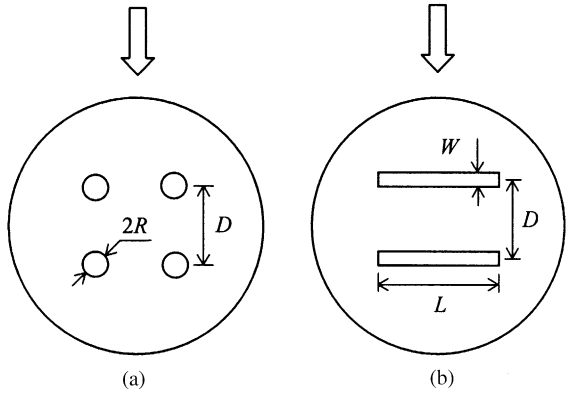


Figure 2. Geometry of the test perforated plates of (a) circular orifices, (b) rectangular orifices; the orifices are square-edged and the plate thickness is $T$. Arrows indicate the direction of grazing flow.

experimental set-up is illustrated in Figure 1. The impedance tube is made of a steel pipe whose inner diameter is 35·0 mm. At one end of the impedance tube is the sound source, which consists of a 50 W loudspeaker. The other end of the impedance tube with a test perforated plate being mounted is exposed to the wind tunnel. The perforated plate is flush with the wall of the wind tunnel. Two B & K 4133 $\frac{1}{2}$ in microphones are installed flush with the inner surface of the impedance tube. Through an A/D coverter, the microphone signals are input into a computer for processing. According to Johnston and Schmidt [23], the acoustic impedance of a sample can be calculated from the amplitudes of and the phase difference between the sound pressures measured by the two microphones.

Grazing flow over the surface of a test perforated plate is introduced through a square-section wind tunnel of internal width 120·0 mm. A Pitot-static tube 3·0 mm in

TABLE 1

*Geometrical parameters of the test perforated plates*

| Number† | $R$ ($L \times W$) (mm) | $T$ (mm) | $N$ | $D$ (mm) | $\sigma$ (%) |
|---|---|---|---|---|---|
| 1 | 3·5 | 0·5 | 1 | — | 4·00 |
| 2 | 3·5 | 2·0 | 1 | — | 4·00 |
| 3 | 1·5 | 2·0 | 4 | 14·0 | 2·94 |
| 4 | 12·0 × 1·0 | 3·0 | 2 | 12·0 | 2·50 |

† Orifices in perforated plates 1–3 are circular, and those in no. 4 are rectangular.

diameter is used to measure the grazing flow speed. Bias flow through the test perforated plate is supplied through the air inlets in the impedance tube at the end of the sound source. A membrane is fixed at the connection of the impedance tube to the sound source in order to prevent air leakage. Bias flow is introduced in two different ways—inflow and outflow. In the inflow case, the airflow is sucked into the impedance tube through the perforated plate, then is expelled into the air by a vacuum pump. In the outflow case, the airflow produced by an air pump goes through the impedance tube and the perforated plate, then flows into the wind tunnel. The airflow is metered by a rotameter, the average flow velocity though the orifices in the test perforated plate is calculated from the measured volume flux.

As shown in Figure 2, the orifices in a test perforated plate are either circular or rectangular. In the case of circular ones, the orifices are arranged in square arrays (a single orifice is located in the center of the perforated plate). For rectangular orifices, the longer side is arranged to be transverse to the grazing flow direction. The geometrical parameters of the four test perforated plates are shown in Table 1.

### 2.2. RELIABILITY TEST OF THE EXPERIMENTAL SET-UP

In the experiment, the radiation resistance of the orifice, into the wind tunnel, is included in the measured data. Cummings and Eversman [18] showed that, at low frequencies, the normalized radiation resistance is equal to $(kR)^2/4$. Under the present experimental conditions, this part of resistance is in the order of $10^{-3}$ or less, thus being of negligible significance in the total acoustic impedance.

When mean flow is absent and the sound pressure level in the impedance tube is low, the normalized specific acoustic reactance of a perforated plate of circular orifices is given by the following equation [16]:

$$x = -\frac{2\pi f}{\sigma c}(1{\cdot}7\,R + T) = C_f\, f, \tag{1}$$

i.e., the normalized specific acoustic reactance is proportional to sound frequency with the coefficient being equal to $-2\pi(1{\cdot}7\,R + T)/\sigma c$. In order to test the reliability of the present experimental set-up, we first carry out an experiment in which the acoustic impedance of the test perforated plates 1–3 is measured on the condition that mean flow is absent and the SPL is low. In Figure 3, the measured normalized specific acoustic reactance of the test perforated plates 1–3 is plotted as a function of sound frequency. The linear variation of the experimental data with sound frequency is clearly demonstrated in this figure. The proportional coefficient $C_f$ can be obtained from the linear fit of the experimental data.

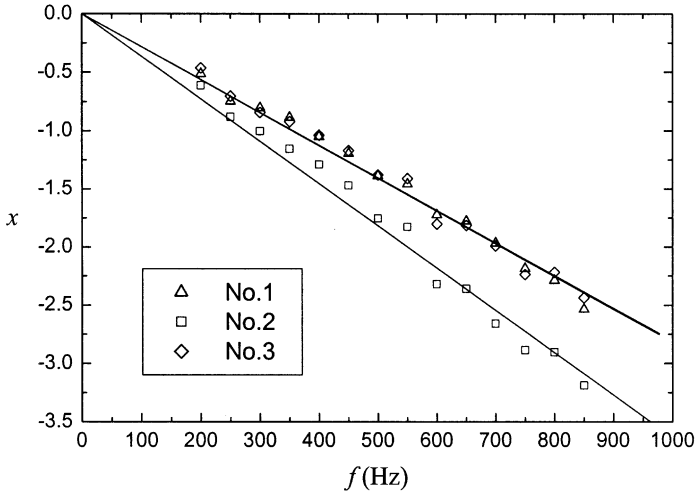


Figure 3. Measured normalized specific acoustic reactance $x$ as a function of sound frequency $f$ for perforated plates 1–3 in conditions of low SPL and zero mean flow; the — indicate the linear fits of the experimental data.

TABLE 2

*Comparison of measured and calculated $C_f$ for test perforated plates* 1–3 *on the condition of low SPL and zero mean flow*

| Number | $C_f$ (measured) | $C_f$ (calculated) | Err (%) |
|---|---|---|---|
| 1 | − 0·00282 | − 0·00294 | 4·1 |
| 2 | − 0·00362 | − 0·00363 | 0·26 |
| 3 | − 0·00281 | − 0·00283 | 0·71 |

In Table 2, the measured coefficients are compared with the values calculated from equation (1). From the comparison we can see that the errors are minor. This result of comparison makes us confident in further carrying out the tests with mean flow.

## 3. EXPERIMENTAL RESULTS

### 3.1. THE CASE OF ZERO GRAZING FLOW OR ZERO BIAS FLOW

#### 3.1.1. *Zero grazing flow case*

When grazing flow is zero, the effect of bias flow on the acoustic impedance of an orifice has been well studied in the previous work. Cummings and Eversman [18] employed linearized Bernoulli equation to explain this bias flow effect. According to reference [18], the normalized specific acoustic resistance of a perforated plate is simply proportional to the average bias flow Mach number through the orifice as below:

$$r = \frac{(1 - \sigma^2 C_v^2)}{\sigma C_v^2} M_B. \tag{2}$$

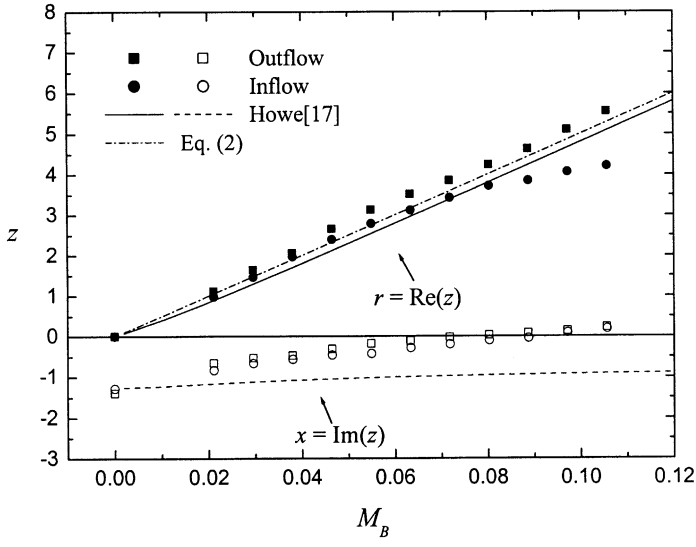


Figure 4. Normalized specific acoustic impedance $z = r + ix$ as a function of bias flow Mach number $M_B$ for perforated plate 1 when grazing flow is zero; $f = 500{\cdot}0$ Hz.

Note that the acoustic resistance given by equation (2) is exactly twice as much as the steady orifice flow resistance $\bar{r} = (1 - \sigma^2 C_v^2)M_B/2\sigma C_v^2$ that is obtained from the whole Bernoulli equation. It is well known that the non-linear acoustic resistance of an orifice at high SPL can be calculated from the steady state resistance to a good approximation. However, in the presence of mean bias flow through the orifice, it is invalid to equate the acoustic resistance to the steady state resistance; and the above analysis indicates that the acoustic resistance is twice as much as the steady flow value.

Figure 4 gives the present experimental data, the calculations of equation (2) and the theoretical results of Howe [17] for perforated plate 1. The *vena contracta* coefficient is taken to be $0{\cdot}7$ that is close to the ideal flow value of $0{\cdot}61$. The minor difference between the two values may be due to the small round-off of the orifice edge which cannot be avoided in the making process of the test perforates. We can see from Figure 4 that the agreement between the experimental and theoretical results is good for the acoustic resistance. As for the acoustic reactance, the absolute value of the experimental data decreases faster than Howe's theoretical results. This over decrease of the reactance may result from the loss of the thickness term at high bias flow speed according to Jing and Sun [20]. In Figure 4, the outflow and inflow experimental results for the resistance are in reasonable agreement, but there is some difference between them at a comparatively high grazing flow speed. The asymmetry of the experimental configuration and the difference of the round-off radius of the two orifice edges may account for the non-coincidence between the outflow and inflow experimental data.

### 3.1.2. *Zero bias flow case*

When bias flow is zero, the grazing flow effect has also received much attention in the previous studies. In Figure 5, the present experiment is compared with the quasi-steady model of Rice [8], the linearized potential flow model of Jing *et al.* [14], and the empirical equation of Lewis and Garrison [21]. Figure 5 shows that the acoustic resistance increases

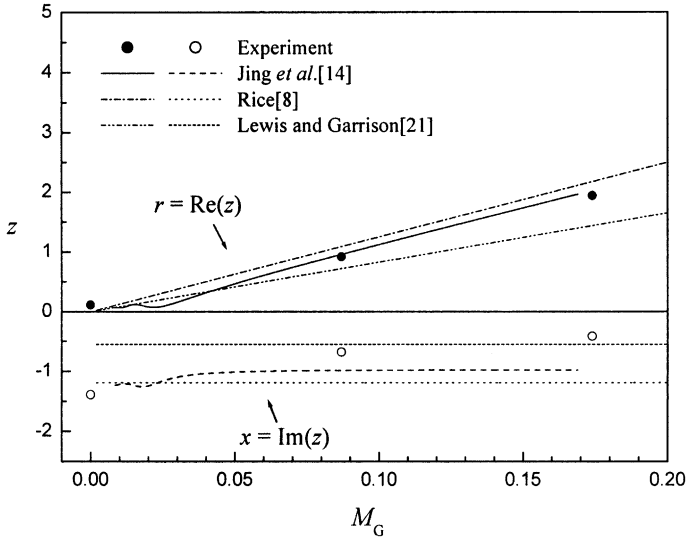


Figure 5. Normalized specific acoustic impedance $z = r + ix$ as a function of grazing flow Mach number $M_G$ for perforated plate 1 when bias flow is zero; $f = 500{\cdot}0$ Hz.

linearly with the increase of grazing flow speed. The proportional coefficient is approximately equal to $0{\cdot}5/\sigma$ according to Rice [8] and Jing *et al.* [14], and $0{\cdot}33/\sigma$ according to Lewis and Garrison [21]. Generally, good agreement is obtained between the present experiment and the previous theories for the acoustic resistance. With respect to the reactance, as grazing flow speed increases, its absolute value decreases and tends to be constant at high grazing flow speed. The decrease of the reactance at high grazing flow speed is well predicted by the empirical model of Lewis and Garrison [21].

### 3.2. GRAZING-INFLOW INTERACTION

In the present experiment, bias flow is produced in two different ways: inflow and outflow. The results of the grazing-inflow interaction are presented in Figures 6–9. These figures show that, in the inflow case, both grazing flow and bias flow have the same effect of increasing the acoustic resistance. It is also seen that grazing flow only has marked influence at very low bias flow speed, and the effect of bias flow dominates at a comparatively high bias flow speed. We perform a simple analysis for the data points in Figures 6–9 that satisfy the condition of $M_G = 0{\cdot}174$ and $M_B > 0{\cdot}1$, in which the value of $|r - r_n|/r_n$ is calculated, where $r_n$ is the corresponding non-grazing flow acoustic resistance. The calculated value is about 10% for perforated plate 1, 4% for no. 2, 8% for no. 3 and 10% for no. 4 respectively. Thus, when $M_B > 0{\cdot}1$, the change of the acoustic resistance due to grazing flow effect is small although the grazing flow speed is much higher than the bias flow speed. Lewis and Garrison [21] have come to the same conclusion that the parallel flow had a negligible effect on the acoustics of a liner if the through flow Mach number is $> 0{\cdot}1$, but whether the through flow is into or out of the liner is not clearly given in reference [21]. Compared with the acoustic resistance, the variation of the acoustic reactance is somewhat irregular. Generally, the absolute value of the acoustic reactance decreases with increase in either grazing flow speed or bias flow speed. In some situations, the acoustic reactance even has positive values at high bias flow speed.

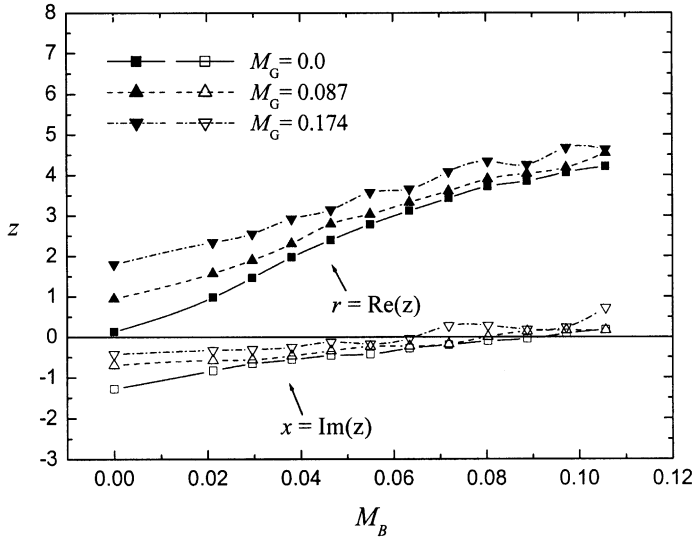


Figure 6. Normalized specific acoustic impedance $z = r + ix$ as a function of bias flow (inflow) Mach number $M_B$ at different grazing flow speeds for perforated plate 1; $f = 500{\cdot}0$ Hz.

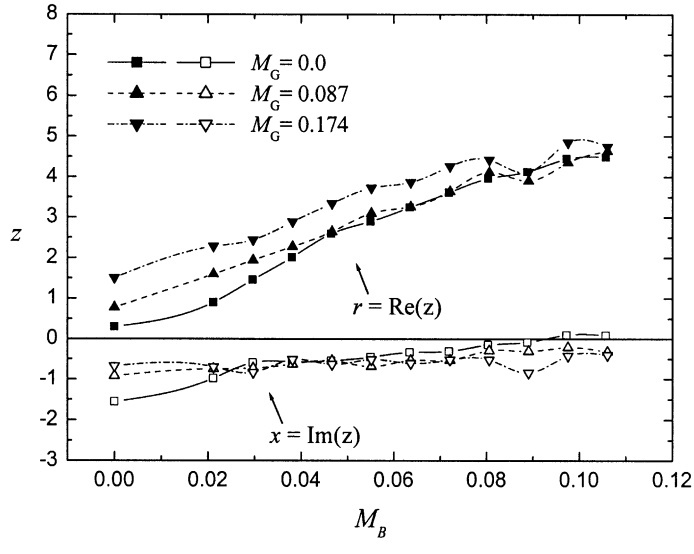


Figure 7. Normalized specific acoustic impedance $z = r + ix$ as a function of bias flow (inflow) Mach number $M_B$ at different grazing flow speeds for perforated plate 2; $f = 500{\cdot}0$ Hz.

The thickness–diameter (width) ratio of the test perforated plates varies from 0·07 to 3·0, but no marked influence of the plate thickness is found from the comparisons of Figures 6–9.

### 3.3. GRAZING–OUTFLOW INTERACTION

The results of the grazing-outflow interaction are presented in Figures 10–13. It is obvious that the outflow experimental results are different from those of the inflow case.

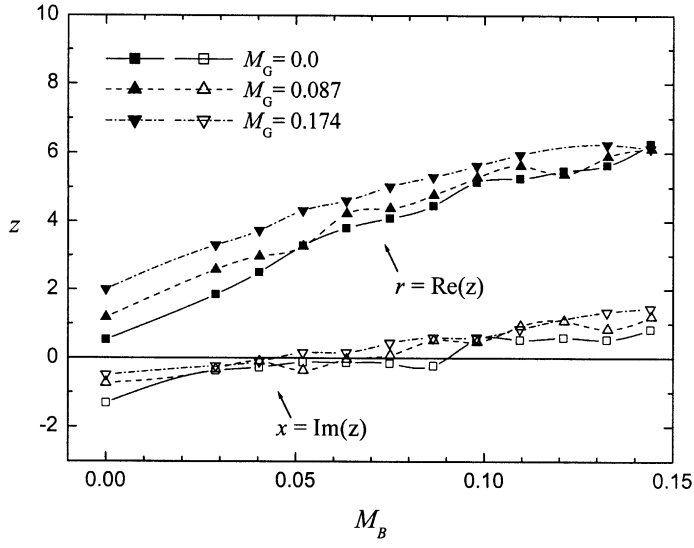


Figure 8. Normalized specific acoustic impedance $z = r + ix$ as a function of bias flow (inflow) Mach number $M_B$ at different grazing flow speeds for perforated plate 3; $f = 500{\cdot}0$ Hz.

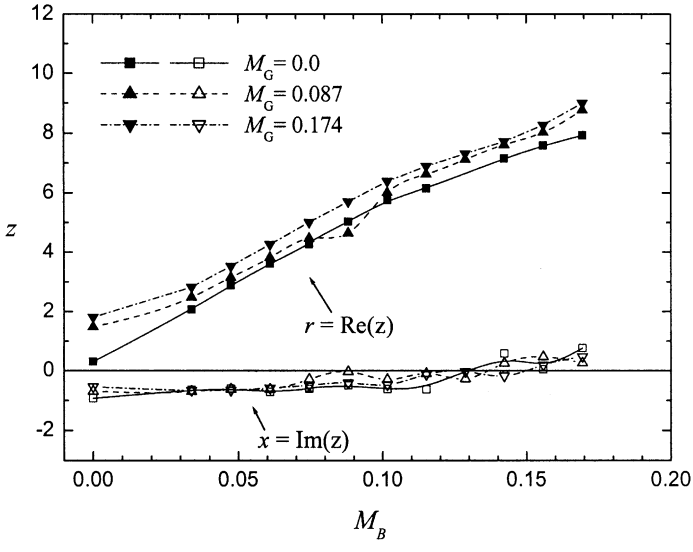


Figure 9. Normalized specific acoustic impedance $z = r + ix$ as a function of bias flow (inflow) Mach number $M_B$ at different grazing flow speeds for perforated plate 4; $f = 250{\cdot}0$ Hz.

One common characteristic of these figures is that, with the increase of grazing flow speed, the acoustic resistance increase at a very low bias flow speed, but gradually drops from the non-grazing flow value at a comparatively high bias flow speed. Take Figure 10 for example. As the grazing flow Mach number increases from zero to 0·087 and 0·174, the acoustic resistance increases from 0·25 (non-grazing flow value) to 0·98 and 1·94 at zero bias flow, but it drops from 5·56 (non-grazing flow value) to 4·99 and 4·32 when bias flow Mach number is 0·105. We call the latter phenomenon "negative grazing flow effect". Similar to

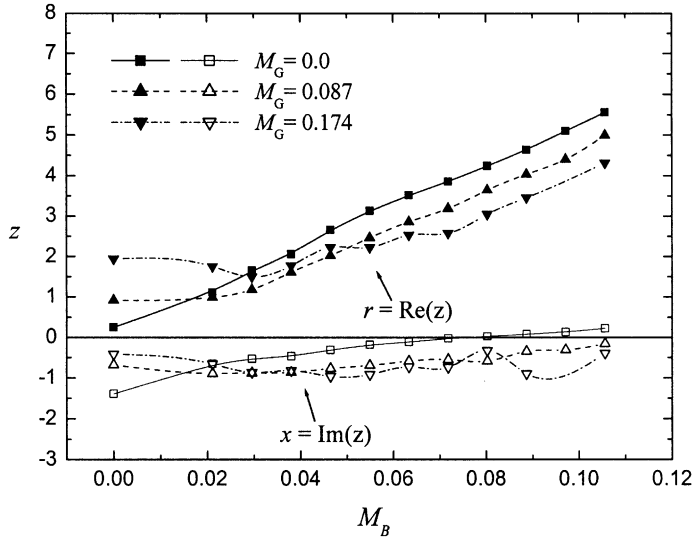


Figure 10. Normalized specific acoustic impedance $z = r + \mathrm{i}x$ as a function of bias flow (outflow) Mach number $M_B$ at different grazing flow speeds for perforated plate 1; $f = 500{\cdot}0$ Hz.

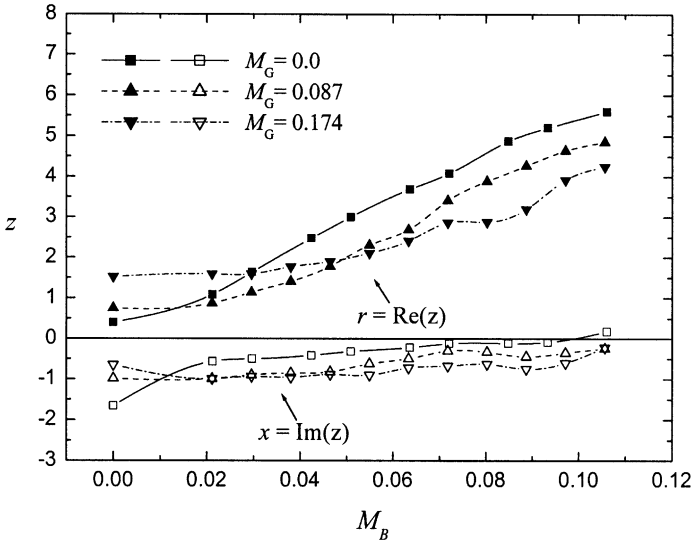


Figure 11. Normalized specific acoustic impedance $z = r + \mathrm{i}x$ as a function of bias flow (outflow) Mach number $M_B$ at different grazing flow speeds for perforated plate 2; $f = 500{\cdot}0$ Hz.

the case of inflow, the variation of the acoustic reactance is somewhat irregular compared with the acoustic resistance. Generally, the absolute value of the acoustic reactance decreases with an increase in either grazing or bias flow speed when the mean flow speed is low. At comparatively high mean flow speed, the acoustic reactance is not markedly affected by both grazing and bias flow, and gradually tends to a constant value.

It is found that the plate thickness has an effect in the grazing-outflow case. The comparison of Figures 10–13 indicates that, as the thickness–diameter (width) ratio

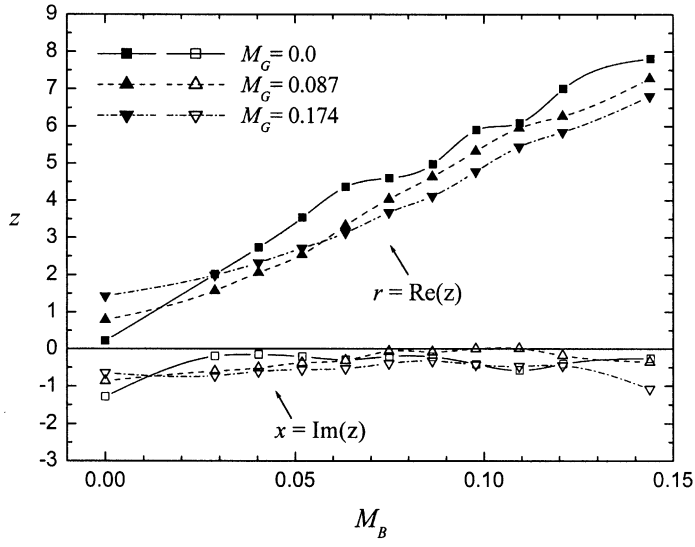


Figure 12. Normalized specific acoustic impedance $z = r + ix$ as a function of bias flow (outflow) Mach number $M_B$ at different grazing flow speeds for perforated plate 3; $f = 500{\cdot}0$ Hz.

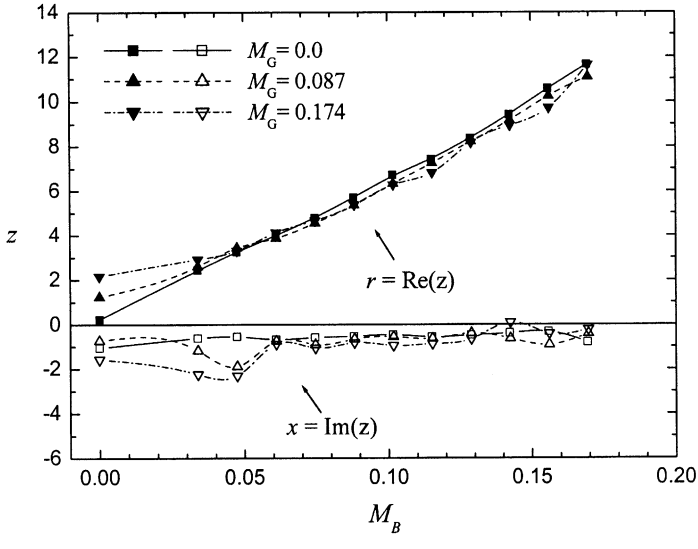


Figure 13. Normalized specific acoustic impedance $z = r + ix$ as a function of bias flow (outflow) Mach number $M_B$ at different grazing flow speeds for perforated plate 4; $f = 200{\cdot}0$ Hz.

increases, the so-called "negative grazing flow effect" is gradually reduced. Among the four test perforated plates, the thickness–width ratio of perforated plate 4 is the largest, and the "negative grazing flow effect" is almost negligible in Figure 13. Note that the orifice in perforate plate 4 is rectangular, thus the orifice shape might also be one of the influential factors.

From the above analysis, we can see that, in both the inflow and outflow cases, the acoustic impedance of a perforated plate depends on the interaction of the two mean flow

conditions rather than a simple summation of the grazing and bias flow effects. Due to grazing flow effect, the acoustic resistance increases slowly with an increase in bias flow speed at high grazing flow speed. Among all the tests carried out, in the case of perforated plate 4 with outflow being present, grazing flow has the least influence on the way that bias flow changes the orifice impedance. Rogers and Hersh [22] have presented an investigation of the interaction between grazing and orifice flow with emphasis on the steady state resistance. The present measured orifice acoustic resistance is compared with the steady state orifice resistance of reference [22], and we find that both kinds of resistance show similar characteristics, such as the difference between grazing-inflow and grazing-outflow interactions, and the so-called "negative grazing flow effect" in the outflow case.

## 4. GRAZING–BIAS FLOW INTERACTION MODEL AND DATA CORRELATION

### 4.1. GRAZING–BIAS FLOW INTERACTION MODEL

A simple fluid dynamic model of the grazing–bias flow interaction is set up in order to provide more insight into the above experimental results. The quasi-steady assumption has been employed in this model, and also a hypothesis is made that the fluctuating velocity due to the sound excitation is far smaller than the mean flow velocity. The previous flow visualization experiments [22, 24] demonstrated that, in the outflow case the orifice flow was deflected downstream while grazing flow was deflected upward, and in the inflow case the flow was drawn into the orifice at a downstream slope; in both cases the orifice jet was characterized by the minimum effective flow area as shown in Figure 14. At this neck of the orifice jet, the flow velocity is almost uniformly distributed and the flow pressure is equal to that of the ambient air. By applying the linearized Bernoulli equation between the orifice jet neck and the far distance into the other side of the orifice plate, the fluctuating pressure difference across the orifice can be approximately written as below:

$$\Delta p = \rho U_C u_C . \tag{3}$$

The effective discharge coefficient is given as follows:

$$C_D = \frac{U_B}{U_C} = \frac{u_O}{u_C}. \tag{4}$$

On the quasi-steady assumption, the normalized specific acoustic resistance of a perforated plate is defined by

$$r = \frac{\Delta p}{\rho c u}. \tag{5}$$

Substituting equations (3) and (4) and the mass continuity relation $u = \sigma u_O$ into equation (5), we obtain the following equation:

$$r = \frac{M_B}{\sigma C_D^2}. \tag{6}$$

Note that equation (6) differs from that for the steady state orifice resistance in reference [22] by a factor of 2. Next, we will try to find the relation between the effective discharge coefficient and the mean flow speeds. As shown in Figure 14(a), it is reasonable to express the velocity $\bar{U}_C$ as the sum of two vectors which are not necessarily normal to each other, and are correspondingly proportional to $U_G$ and $U_B$ in magnitude. Therefore, $U_C$ is

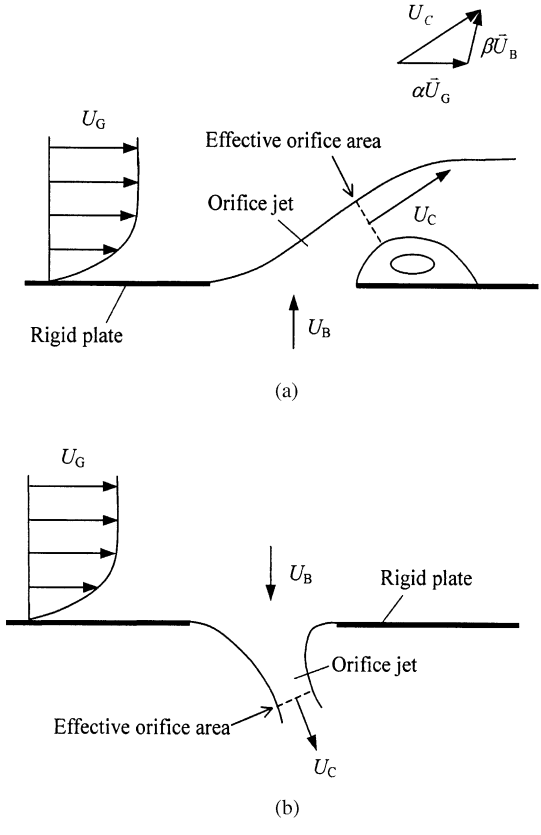


Figure 14. Schematic of grazing–bias flow interaction model: (a) Outflow; (b) inflow.

generally related to $U_G$ and $U_B$ as follows:

$$U_C = \sqrt{k_1 U_B^2 + k_2 U_B U_G + k_3 U_G^2}. \tag{7}$$

From equations (4) and (7), we can obtain

$$C_D = \frac{1}{\sqrt{k_1 + k_2/j + k_3/\lambda^2}}. \tag{8}$$

The proportionality factors $k_1$, $k_2$ and $k_3$ in equations (7) and (8) will be determined in the next subsection.

### 4.2. DATA CORRELATION

Equation (8) indicates that the effective discharge coefficient depends only on the ratio of the bias flow speed to grazing flow speed. By the use of equation (6), the effective discharge coefficient can be obtained from the measured acoustic resistance. In Figure 15, $C_D$ is plotted against $M_B/M_G$. The difference between the outflow and inflow data of the acoustic resistance suggests that $C_D$ should be individually correlated for the two cases. We can see

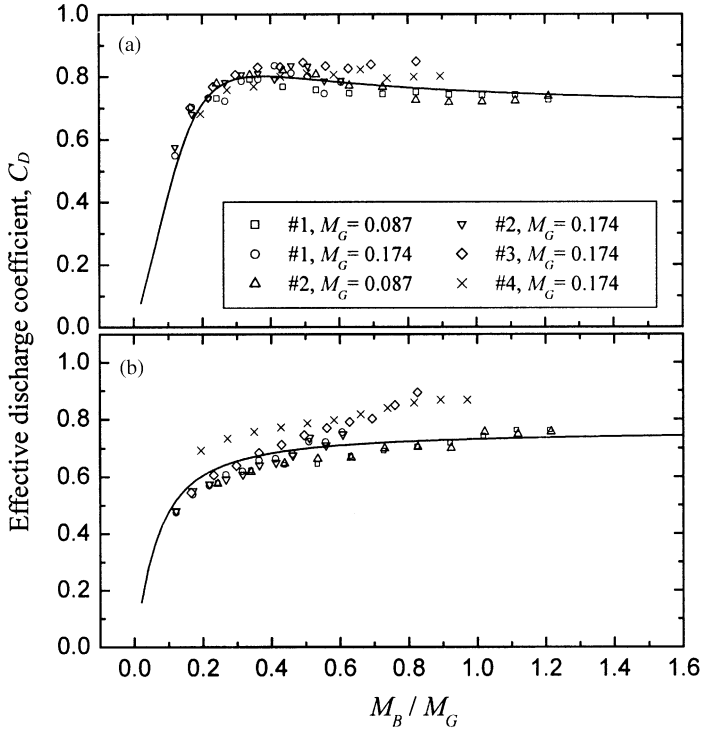


Figure 15. Effective discharge coefficient as a function of the ratio of bias flow Mach number to grazing flow Mach number, the —— curves are calculated from equations (8) and (9): (a) Outflow; (b) inflow.

from Figure 15 that, generally a good correlation of the data is obtained for outflow whereas there is much scattering in the data for inflow. According to Rogers and Hersh [22], for the steady-state orifice resistance the plate thickness has a far greater effect on the data correlation in the inflow case than in the outflow case. Taking advantage of the close connection between the steady state and acoustic resistance, we think that the influence of plate thickness may account for the data scattering in Figure 15(b). It can be noted that the thickness–diameter (width) ratios of perforated plates 3 and 4 is much larger than those of no. 1 and no. 2, so the data for perforated plates 3 and 4 is not correlated well with those of no. 1 and no. 2 in Figure 15(b). Besides, different from nos. 1–3, the perforated plate 4 has rectangular orifices of large length–width ratio; so the orifice shape may also influence the data correlation for the effective discharge coefficient.

The plate thickness effect has not been incorporated into the grazing–bias flow interaction model. Therefore, in Figure 15 equation (8) is fitted to the data for perforated plates 1 and 2 whose thickness–diameter ratios have small values of 0·07 and 0·29 respectively. Then, the following empirical values for the proportionality factors in equation (8) are obtained:

$$\begin{aligned} k_1 &= 2{\cdot}10, \quad k_2 = -0{\cdot}332, \quad k_3 = 0{\cdot}0556 \quad \text{(for outflow)}, \\ k_1 &= 1{\cdot}72, \quad k_2 = +0{\cdot}138, \quad k_3 = 0{\cdot}0127 \quad \text{(for inflow)}. \end{aligned} \tag{9}$$

As shown in Figure 15, the outflow $C_D$ curve first increases markedly, reaches its maximum value when $M_B/M_G$ is about 0·3, and then decreases slightly with the increase of $M_B/M_G$; in

contrast, the inflow $C_D$ curve always increases with increasing $M_B/M_G$. It is found that the change tendency of the $C_D$ curves in Figure 15 is quite similar to that for the steady state orifice resistance given by Rogers and Hersh [22]. Evidently, the decrease of the outflow $C_D$ when $M_B/M_G > 0{\cdot}3$ corresponds to the drop of the acoustic resistance below the non-grazing flow value when high-speed outflow interacts with grazing flow.

## 5. CONCLUSIONS

In this paper, the acoustic behavior of a perforated plate subjected to grazing–bias flow interaction is investigated. It is concluded that:

(1) Grazing-inflow and grazing-outflow interactions have different effects on the orifice acoustic resistance. In the outflow case, grazing flow results in the drop of the acoustic resistance below the non-grazing flow value at a comparatively high bias flow speed, whereas it generally has the effect of increasing the acoustic resistance in the inflow case.

(2) Compared with the acoustic resistance, the variation of the acoustic reactance is somewhat irregular. Generally, the absolute value of the acoustic reactance decreases with the increase of either grazing or bias flow speed when mean flow speed is low. At a comparatively high mean flow speed, the acoustic reactance is not markedly affected by both grazing and bias flow, and gradually tends to a constant value.

(3) Due to grazing flow effect, the acoustic resistance of an orifice increases slowly with the increase of bias flow speed, but the acoustic resistance is dominated by the bias flow effect when bias flow speed is comparatively high. In the inflow case, when bias flow Mach number is $> 0{\cdot}1$, grazing flow effect is almost negligible. Among all the tests carried out, in the case of rectangular orifice of large thickness–width ratio with outflow being present, grazing flow has the least influence on the way bias flow changes the acoustic impedance.

(4) A simple grazing–bias flow interaction model is set up to explain the observed phenomena. This model shows that the acoustic resistance of an orifice in a thin plate is proportional to bias flow Mach number, and is inverse to the square of the effective discharge coefficient $C_D$ which can be expressed as follows:

$$C_D = \frac{1}{\sqrt{k_1 + k_2/\lambda + k_3/\lambda^2}},$$

where $\lambda$ is the ratio of bias flow speed to grazing flow speed. It is found that the above equation fits well with the experimental data when the proportionality factors $k_1$, $k_2$ and $k_3$ have the empirical values of 2·10, $-0{\cdot}332$ and 0·0566 for outflow or 1·72, 0·138 and 0·0127 for inflow respectively.

## ACKNOWLEDGMENTS

The sponsorship of the National Natural Science Foundation of China (59925616) and the Aeronautical Science Foundation of China (00C51040) is greatly acknowledged.

## REFERENCES

1. P. D. DEAN and B. J. TESTER 1975 *NASA* CR-134998. Duct wall impedance control as an advanced concept for acoustic suppression.
2. X. SUN and S. KAJI 2000 *American Institute of Aeronautics and Astronautics Journal* **38**, 1525–1533. Effect of wall admittance changes on aeroelastic stability of turbomachines.

3. X. SUN, X. JING and H. ZHAO 2001 *Journal of Propulsion and Power* **17**, 248–255. Control of blade flutter by smart casing treatment.
4. J. HUGHES and A. P. DOWLING 1990 *Journal of Fluid Mechanics* **218**, 299–335. The absorption of sound by perforated linings.
5. H. ZHAO and X. SUN 1999 *American Institute of Aeronautics and Astronautics Journal* **37**, 825–831. Active control of wall acoustic impedance.
6. H. W. KWAN, J. YU, B. BEER and D. ARMITAGE 1999 *AIAA Paper* 99-1939. Bias flow adaptive acoustic liner.
7. P. CATALDI, K. AHUJA and R. GAETA Jr. 1999 *AIAA Paper* 99-1879. Enhanced sound absorption through negative bias flow.
8. E. J. RICE 1976 *NASA* TM X-71903. A theoretical study of the acoustic impedance of orifices in the presence of a steady grazing flow.
9. J. KOMPENHANS and D. RONNEBERGER 1980 *AIAA Paper* 80-0990. The acoustic impedance of the orifices in the plate of a flow duct with a laminar or turbulent flow boundary layer.
10. B. E. WALKER and A. F. CHARWAT 1982 *Journal of the Acoustical Society of America* **72**, 550–555. Correlation of the effects of grazing flow on the impedance of helmholtz resonators.
11. A. CUMMINGS 1986 *Acustica* **61**, 233–242. The effects of grazing turbulent pipe-flow on the impedance of an orifice.
12. M. S. HOWE, M. I. SCOTT and S. R. SIPCIC 1996 *Proceedings of the Royal Society of London, Series* A **452**, 2303–2317. The influence of tangential mean flow on the Rayleigh conductivity of an aperture.
13. M. S. HOWE 1997 *Journal of Fluids and Structures* **11**, 351–366. Influence of plate thickness on Rayleigh conductivity and flow-induced aperture tones.
14. X. JING, X. SUN, J. WU and K. MENG 2001 *American Institute of Aeronautics and Astronautics Journal* **39**, 1478–1484. Effect of grazing flow on the acoustic impedance of an orifices.
15. D. W. BECHERT 1980 *Journal of Sound and Vibration* **70**, 389–405. Sound absorption caused by vorticity shedding demonstrated with a jet flow.
16. U. INGARD and H. ISING 1967 *Journal of the Acoustical Society of America* **42**, 6–17. Acoustic nonlinearity of an orifice.
17. M. S. HOWE 1979 *Proceedings of Royal Society of London*, A **366**, 205–223. On the theory of unsteady high reynolds number flow through a circular aperture.
18. A. CUMMINGS and W. EVERSMAN 1983 *Journal of Sound and Vibration* **91**, 503–518. High amplitude acoustic transmission through duct terminations: theory.
19. M. SALIKUDDIN and K. K. AHUJA 1983 *Journal of Sound and Vibration* **91**, 479–502. Acoustic power dissipation on radiation through duct terminations: experiments.
20. X. JING and X. SUN 2000 *American Institute of Aeronautics and Astronautics Journal* **38**, 1573–1578. Effect of plate thickness on impedance of perforated plates with bias flow.
21. G. D. LEWIS and G. D. GARRISON 1971 *AIAA Paper* 71-699. The role of acoustic absorbers in preventing combustion instability.
22. T. ROGERS and A. S. HERSH 1975 *AIAA Paper* 75-493. The effect of grazing flow on the steady state resistance of square-edged orifices.
23. J. P. JOHNSTON and W. E. SCHMIDT 1978 *Journal of the Acoustical Society of America* **63**, 1455–1460. Measurement of acoustic reflection from an obstruction in a pipe with flow.
24. K. J. BAUMEISTER and E. J. RICE 1975 *NASA* TM X-3288. Visual study of the effect of grazing flow on the oscillatory flow in a resonator orifice.

## APPENDIX A: NOMENCLATURE

| | |
|---|---|
| $c$ | sound speed |
| $C_D$ | effective discharge coefficient |
| $C_f$ | $-2\pi(1{\cdot}7R + T)/\sigma c$ |
| $C_v$ | *vena contracta* coefficient |
| $D$ | spacing between orifices |
| $f$ | sound frequency |
| $i$ | $\sqrt{-1}$ |
| $k$ | sound wave number |
| $L$ | length of a rectangular orifice |
| $M_B$ | average bias flow Mach number through an orifice, $U_B/c$ |

| | |
|---|---|
| $M_G$ | grazing flow Mach number over a perforated plate, $U_G/c$ |
| $N$ | number of orifices in a perforated plate |
| $\Delta p$ | fluctuating pressure difference across an orifice |
| $r$ | normalized acoustic resistance of a perforated plate by $\rho c$ |
| $\bar{r}$ | normalized steady state resistance of an orifice plate by $\rho c$ |
| $R$ | orifice radius |
| $T$ | plate thickness |
| $u$ | normal fluctuating velocity on the surface of a perforated plate |
| $u_O$ | average fluctuating velocity through an orifice |
| $u_C$ | fluctuating velocity on the orifice effective area |
| $U_C$ | mean flow velocity on the orifice effective area |
| $U_B$ | average bias flow speed through an orifice |
| $U_G$ | grazing flow speed over a perforated plate |
| $W$ | width of a rectangular orifice |
| $x$ | normalized acoustic reactance of a perforated plate by $\rho c$ |
| $z$ | normalized specific acoustic impedance of a perforated plate by $\rho c$, $\mathrm{r} + \mathrm{i}x$ |
| $\lambda$ | ratio of bias flow speed to grazing flow speed, $M_B/M_G$ |
| $\rho$ | air density |
| $\sigma$ | open area ratio |